Materials Science and Engineering A 527 (2010) 2951–2961

Contents lists available at ScienceDirect

Materials Science and Engineering A

journal homepage: www.elsevier.com/locate/msea

Tensile properties and strain-hardening behavior of double-sided arc welded and friction stir welded AZ31B magnesium alloy

S.M. Chowdhury[a], D.L. Chen[a,*], S.D. Bhole[a], X. Cao[b], E. Powidajko[c], D.C. Weckman[c], Y. Zhou[c]

[a] Department of Mechanical and Industrial Engineering, Ryerson University, 350 Victoria Street, Toronto, Ontario M5B 2K3, Canada
[b] Aerospace Manufacturing Technology Centre, Institute for Aerospace Research, National Research Council Canada, 5145 Decelles Avenue, Montreal, Quebec H3T 2B2, Canada
[c] Department of Mechanical and Mechatronics Engineering, University of Waterloo, 200 University Avenue West, Waterloo, Ontario N2L 3G1, Canada

ARTICLE INFO

Article history:
Received 17 November 2009
Received in revised form 8 January 2010
Accepted 11 January 2010

Keywords:
AZ31 magnesium alloy
Double-sided arc welding
Friction stir welding
Microstructure
Tensile properties
Strain hardening

ABSTRACT

Microstructures, tensile properties and work hardening behavior of double-sided arc welded (DSAWed) and friction stir welded (FSWed) AZ31B-H24 magnesium alloy sheet were studied at different strain rates. While the yield strength was higher, both the ultimate tensile strength and ductility were lower in the FSWed samples than in the DSAWed samples due to welding defects present at the bottom surface in the FSWed samples. Strain-hardening exponents were evaluated using the Hollomon relationship, the Ludwik equation and a modified equation. After welding, the strain-hardening exponents were nearly twice that of the base metal. The DSAWed samples exhibited stronger strain-hardening capacity due to the larger grain size coupled with the divorced eutectic structure containing β-$Mg_{17}Al_{12}$ particles in the fusion zone, compared to the FSWed samples and base metal. Kocks–Mecking type plots were used to show strain-hardening stages. Stage III hardening occurred after yielding in both the base metal and the welded samples. At lower strains a higher strain-hardening rate was observed in the base metal, but it decreased rapidly with increasing net flow stress. At higher strains the strain-hardening rate of the welded samples became higher, because the recrystallized grains in the FSWed and the larger re-solidified grains coupled with β particles in the DSAWed provided more space to accommodate dislocation multiplication during plastic deformation. The strain-rate sensitivity evaluated via Lindholm's approach was observed to be higher in the base metal than in the welded samples.

1. Introduction

Weight reduction in ground vehicles and aircraft is one of the important measures to improve fuel economy and protect the environment [1]. Magnesium alloys, as the lightest metallic structural alloys, have been and will be increasingly used in the automotive and aerospace industries due to their low density [1], high strength-to-weight ratio [1–3], environmental friendliness, recyclability and castability [2,3]. However, effective joining techniques are required to further expand the applications of magnesium alloys.Friction stir welding (FSW), a solid-state joining technique developed by The Welding Institute of Cambridge, UK, in 1991 [4], has great potential for joining magnesium alloys, since it can significantly reduce weld defects normally associated with fusion welding processes [1,5]. FSW has also been used to refine the grain size via severe plastic deformation and recrystallization [6–9] so as to improve the workability of Mg alloys and increase the strength of welded joints. On the other hand, the weldability of magnesium alloys by some arc welding processes such as gas tungsten arc welding (GTAW) is considered to be excellent as well [10]. In 1999, Zhang and Zhang [11] developed and patented a novel arc welding process referred to as double-sided arc welding (DSAW). The DSAW process uses one welding power supply and two torches; frequently a plasma arc welding (PAW) and GTAW torch each connected directly to one of the power supply terminals. The torches are positioned on opposite sides of a work-piece such that the welding current flows from one torch through the work-piece to the opposite torch. Zhang et al. [12–15] have examined the feasibility of using the DSAW process to make vertical-up, keyhole-mode welds in 6–12 mm thick plain carbon steel, stainless steel or aluminum alloy plates. More recently, Weckman and co-workers [16,17] have examined the feasibility of using the DSAW process for conduction-mode welding of 1.2 mm thick AA5182-O aluminum sheet for tailor welded blank applications. It was noted that the opposing welding torches and square-wave AC welding current successfully cleaned the oxide from both sides of the joint and produced visually acceptable welds at speeds up to 3.6 m/min. Through-thickness heating was more uniform with DSAW than with other single-sided welding processes allowing symmetric welds to be produced with minimal angular distortion of the sheets [16,17].

* Corresponding author. Tel.: +1 416 979 5000x6487; fax: +1 416 979 5265.
E-mail address: dchen@ryerson.ca (D.L. Chen).

0921-5093/$ – see front matter © 2010 Elsevier B.V. All rights reserved.
doi:10.1016/j.msea.2010.01.031

Mechanical properties such as strength, ductility, strain-hardening behavior, strain-hardening sensitivity, etc., of all welds made in magnesium alloy parts used in structural applications must be evaluated to ensure the integrity and safety of the joint and structure. While there are numerous investigations on the properties of magnesium alloys, only a limited number of studies of the properties of welded magnesium alloy joints are reported. Quan et al. [18] studied the effects of heat input on microstructure and tensile properties of laser welded AZ31 Mg alloy. Liu and Dong [19] reported the effect of microstructural changes on the tensile properties in non-autogenous gas tungsten arc welded AZ31 magnesium alloy. Zhu et al. [20] presented the effect of welding parameters on the welding defects and change of microstructure in CO_2 and diode laser welded AZ31 magnesium alloy. Tensile testing has also been done on friction stir welded AZ31 [1,5,21–24], FSWed wrought AZ61 [25] and a fine-grained laser welded Mg alloy [26]. Some earlier results on the microstructural changes and strengths of various FSWed magnesium alloys and other alloys have also been well documented (e.g., in refs. [27–29]). Takuda et al. [30] performed tensile tests on a Mg–9Li–1Y alloy at room temperature and observed that the values of strain-hardening exponents increased with increasing strain rate. Afrin et al. [24] obtained similar results for a FSWed AZ31B-H24 Mg alloy. Yu et al. [31] evaluated the tensile strength of FSWed thixomolded AE42 Mg alloy, but no information on strain-hardening and strain-rate sensitivity was given, while Lee et al. [32] studied the formability of friction stir welded AZ31 magnesium alloy sheet and other alloys experimentally and numerically. Some authors have studied the strain-hardening behavior of magnesium alloys with emphasis on the relationships between the grain size strengthening and dislocation strain hardening of the material [2,24,33–35]. While Shen et al. [36] have evaluated the formation of macropores in double-sided gas tungsten arc welded wrought magnesium AZ91D alloy plates made with two separate passes (i.e., welded with one partial penetration weld on the top side and then a separate partial penetration weld on the back side of the plate), the mechanical properties of conduction-mode double-sided arc welds made in magnesium alloy sheet have not been examined. It is unknown if this novel arc welding technique could be used to produce welds in magnesium alloys with acceptable mechanical properties. The aim of the present investigation, therefore, was to evaluate and compare the microstructure, tensile properties, strain-hardening and strain-rate sensitivity of DSAWed and FSWed AZ31B-H24 Mg alloy sheet.

2. Materials and experimental procedure

In the present study, 2 mm thick AZ31B-H24 Mg alloy sheet was used. The nominal chemical composition of this alloy was 2.5–3.5 wt% Al, 0.7–1.3 wt% Zn, 0.2–1.0 wt% Mn and balance Mg [37]. Two different welding methods, DSAW and FSW, were employed to make autogenous welds between the work-pieces in the butt joint configuration. Both DSAWed and FSWed joints were made with the welding direction perpendicular to the rolling direction of the sheet. In the DSAW process, a PAW torch and a GTAW torch were used with a square-wave AC welding power supply. A detailed description of the welding apparatus and other process parameters used may be found in [16,17]. Prior to DSAW, the work-pieces were degreased using acetone and then alcohol. The oxide on the surface of the sheets was then mechanically removed in the area of the weld using a stainless steel wire brush. The DSAW welds were made using a welding speed of 25 mm/s and welding power of 1.4 kW. The FSW welds were made using a welding speed of 10 mm/s and a right-hand threaded pin tool having a pin length of 1.65 mm rotating clockwise at a rate of 2000 rpm. Prior to FSW, surface oxides were removed with a steel brush and then the surface was cleaned using ethanol as well.

The welded joints perpendicular to the welding direction were cut and cold mounted in order to examine the microstructure of the fusion zone (FZ), heat-affected zone (HAZ) and base metal (BM). The mounted samples were manually ground, polished, and etched using acetic picral (10 mL acetic acid (99%), 4.2 g picric acid, 10 mL H_2O, 70 mL ethanol (95%)) [38]. The microstructure was observed with an optical microscope equipped with quantitative image analysis software. Vickers microhardness tests were conducted with a computerized Buehler machine across the sectioned weld with a spacing of 0.5 mm. A load of 100 g and dwell time of 15 s were applied during the hardness tests. Sub-sized tensile specimens in accordance with ASTM E8M-08 standard [39] were machined along the rolling (or longitudinal) direction for both the base metal and welded joints, where the weld was positioned at the center of the gauge area. Tensile tests were performed using a computerized tensile testing machine at constant strain rates of 1×10^{-2}, 1×10^{-3}, 1×10^{-4} and 1×10^{-5} s^{-1} at room temperature. At least two samples were tested at each strain rate. The fracture surfaces were examined using a scanning electron microscope (SEM) equipped with an energy dispersive X-ray spectroscopy (EDS) system and 3D fractographic analysis capacity.

3. Results and discussion

3.1. Microstructure

The microstructure of the AZ31B-H24 Mg base metal is shown in Fig. 1, where elongated and pancake-shaped grains with varying sizes were observed. The heterogeneity in the grain structure of the base metal was due to both deformation of the 2 mm thick sheet by rolling and incomplete dynamic recrystallization (partial annealing) [1]. The average grain size of the base metal was about 5 μm. The typical macroscopic and microscopic structures of FSWed AZ31B-H24 Mg alloys are shown in Fig. 2. Fig. 2(a) shows the top weld bead after FSW and Fig. 2(b) presents a typical cross-section of the FSWed sample including HAZ, thermomechanically affected zone (TMAZ) and stir zone (SZ). As seen in Fig. 2(c), both equiaxed and elongated grains were present in the HAZ. However, in comparison to the base metal (Fig. 1), far more equiaxed grains appeared in the HAZ, indicating that partial recrystallization had also taken place during FSW. The recrystallization temperature of the alloy was approximately 205 °C. Thus, the temperature in part of the HAZ may have been above this value. This is confirmed by some large grains observed in the HAZ due to grain growth after recrystallization [1]. The grain structure in the TMAZ (Fig. 2(d)) in the present study is basically equiaxed and recrystallized, which

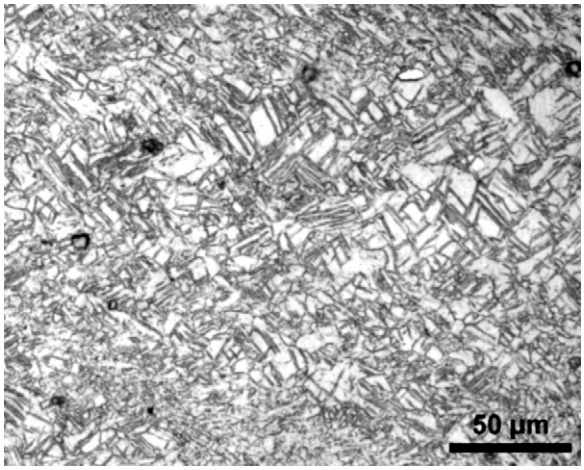

Fig. 1. Typical microstructures of the base metal (BM) of the AZ31-H24 Mg alloy.